

A. LISIŃSKA-CZEKAJ<sup>1\*</sup>, D. CZEKAJ<sup>1</sup>, B. GARBARZ-GLOS<sup>2</sup>,  
W. BĄK<sup>2</sup>, I. KUŹNIARSKA-BIERNACKA<sup>3</sup>

## X-RAY DIFFRACTION STUDY OF BISMUTH LAYER-STRUCTURED MULTIFERROIC CERAMICS

Goal of the present research was to apply a solid state reaction route to fabricate bismuth layer-structured multiferroic ceramics described with the formula  $\text{Bi}_5\text{FeTi}_3\text{O}_{15}$  and reveal the influence of processing conditions on its crystal structure and phase composition. Simple oxide powders  $\text{Bi}_2\text{O}_3$ ,  $\text{TiO}_2$  and  $\text{Fe}_2\text{O}_3$  were used to fabricate Aurivillius-type bismuth layer-structured ferroelectrics. Pressureless sintering in ambient air was employed and the sintering temperature was  $T_S = 900^\circ\text{C}$ ,  $T_S = 1000^\circ\text{C}$  and  $T_S = 1040^\circ\text{C}$ . The phase composition as well as crystal structure of ceramics sintered at various processing conditions was examined with powder X-ray diffraction method at room temperature. The Rietveld refinement method was applied for analysis of X-ray diffraction data. It was found that ceramics adopted orthorhombic structure  $Cmc21$ . The unit cell parameters of bismuth layer-structured multiferroic ceramics increased slightly with an increase in sintering temperature.

*Keywords:*  $\text{Bi}_5\text{FeTi}_3\text{O}_{15}$  ceramics, X-ray diffraction, crystal structure

### 1. Introduction

Bismuth layer-structured ferroelectrics (BLSF) are of great technological interest because of their applications as non-volatile ferroelectric memories [1,2], and high-temperature piezoelectric materials [3]. This is mainly because BLSF have high-fatigue resistance [2], high-Curie temperature, low dielectric loss, and high-dielectric breakdown strength [4]. If modified appropriately, BLSF may exhibit novel physical properties which enrich their functionality [5,6]. For instance, BLSF materials of  $\text{Bi}_4\text{Ti}_3\text{O}_{12}$ - $\text{BiFeO}_3$  (BTO-BFO) system, are characterized in that they combine ferroelectric, semiconducting and ferromagnetic properties. Therefore, they are potentially attractive for information processing as well as information storage applications [7].

The general formula of BTO-BFO compounds is  $\text{Bi}_{m+1}\text{Fe}_{m-3}\text{Ti}_3\text{O}_{3m+3}$  [8]. They exhibit a non-trivial crystal structure which was first described by Aurivillius [e.g. 9]. A layered perovskite-like structure consists of fluorite-like bismuth-oxygen layers of  $\{(\text{Bi}_2\text{O}_2)^{2+}\}_\infty$  that alternate with (001) perovskite-like slabs  $\{(\text{Bi}_{m+1}\text{Fe}_{m-3}\text{Ti}_3\text{O}_{3m+1})^{2-}\}_\infty$ . The values of  $m$  indicates the number of perovskite-like layers per slab and may take integer or fractional values. Fractional  $m$  value corresponds to

mixed-layer structures [10], which contain perovskite slabs of different thicknesses. Among the Aurivillius-type compounds  $\text{Bi}_5\text{FeTi}_3\text{O}_{15}$  ( $m = 4$  oxygen octahedra in the perovskite-like slabs) has a four-layered perovskite units of nominal composition  $(\text{Bi}_3\text{FeTi}_3\text{O}_{13})^{2-}$  sandwiched by neighboring two  $(\text{Bi}_2\text{O}_2)^{2+}$  layers along the  $c$ -axis in a unit cell.

Several research studies have been devoted to characterization of  $\text{Bi}_5\text{FeTi}_3\text{O}_{15}$  compound [e.g. 1,6,11]. In that connection it is worth to mention our earlier studies also [e.g. 12-14]. A brief description of the crystal structure and multiferroic properties of BFTO ( $m = 4$ ) can be summarized as follows.

According to the published crystallographic data  $\text{Bi}_5\text{FeTi}_3\text{O}_{15}$  compound exhibits an orthorhombically distorted Aurivillius-type crystal structure which can be described well by  $A21am$  [15], or  $Cmc21$  [12] space group (SG) – these are different settings of the same SG No 36. There are also possible crystal structures of  $\text{Bi}_5\text{FeTi}_3\text{O}_{15}$  described by  $Fmm2$  (SG No 42) [16] or  $Pnn2$  (SG No 32) at room temperature. BFTO ( $m = 4$ ) is known to show a relatively high resistivity at room temperature. The  $(\text{Bi}_2\text{O}_2)^{2+}$  layers play key roles as both space-charge compensation and insulation, which are expected to reduce the leakage current [17]. At room temperature, the remnant polariza-

<sup>1</sup> GDANSK UNIVERSITY OF TECHNOLOGY, FACULTY OF MECHANICAL ENGINEERING, DEPARTMENT OF MATERIALS ENGINEERING AND WELDING, 11/12, NARUTOWICZA STR., 80-233 GDANSK, POLAND

<sup>2</sup> PEDAGOGICAL UNIVERSITY OF CRACOW, INSTITUTE OF TECHNOLOGY, 2 PODCHORĄŻYCH STR., 30-084 KRAKÓW, POLAND

<sup>3</sup> REQUIMTE/LAQV, DEPARTAMENTO DE QUÍMICA E BIOQUÍMICA, FACULDADE DE CIÊNCIAS, UNIVERSIDADE DO PORTO, RUA DO CAMPO ALEGRE S/N, 4169-007 PORTO, PORTUGAL

\* Corresponding author: agata.czekaj@pg.edu.pl



tion and the coercive field of  $\text{Bi}_5\text{FeTi}_3\text{O}_{15}$  samples were about  $2P_r = 11.8 \mu\text{C}/\text{cm}^2$  and  $2E_c = 270 \text{ kV}/\text{cm}$ , respectively. The BFTO samples show a weak ferromagnetism with  $M \approx 1.36 \times 10^{-6} \text{ emu}/\text{g}$  [18]. A ferroelectric-paraelectric phase transition was determined to be about  $T = 730^\circ\text{C}$  corresponding to a structural transition from the  $A21am$  to the  $I4/mmm$ .  $\text{Bi}_5\text{FeTi}_3\text{O}_{15}$  is antiferromagnetic with a Néel temperature of  $T = -193^\circ\text{C}$  (80 K). Moreover, its magnetoelectric (ME) properties were also investigated recently, and the values of the first-order and second-order ME coefficients are  $\alpha_{\text{ME}} = 0.1 \text{ mVcm}^{-1}\text{Oe}^{-1}$  and  $\beta_{\text{ME}} = 37 \times 10^{-5} \text{ mVcm}^{-1}\text{Oe}^{-2}$ , respectively [17].

Aim of the present research was to synthesize  $\text{Bi}_5\text{FeTi}_3\text{O}_{15}$  compound which is a member of the BTO-BFO system with  $m = 4$  perovskite-like layers, and manufacture BFTO ( $m = 4$ ) ceramics at various processing conditions (i.e. sintering temperature and sintering time) to study the evolution of the phase composition, exhibited crystal structure, and degree of perfection of the crystal structure in terms of average crystal size and average lattice strain as well as the Rietveld fitting parameters.

## 2. Experimental

The route called mixed oxide method was employed for fabrication of  $\text{Bi}_5\text{FeTi}_3\text{O}_{15}$  ceramics. Simple oxide powders  $\text{Bi}_2\text{O}_3$ ,  $\text{TiO}_2$  and  $\text{Fe}_2\text{O}_3$  were used for stoichiometric mixture preparation. Parameters of the thermal treatment were determined by simultaneous thermal analysis (DTA/TG/DTG) [12,14]. After calcinations ( $T_{\text{calc}} = 720^\circ\text{C}$ ) the pellets were formed and pressed into disks with the diameter of 10 mm and 1 mm thickness. Pressureless sintering was used for final densification of ceramic samples. Sintering temperatures were  $T_s = 900^\circ\text{C}$ ,  $T_s = 1000^\circ\text{C}$ , and  $T_s = 1040^\circ\text{C}$  whereas the soaking time was  $t_s = 2 \text{ h}$  in the first experiment and  $t_s = 24 \text{ h}$  in the last two experiment sets.

The crystal structure of BFTO ceramics were studied by X-ray diffraction method at room temperature (XPert-Pro diffractometer,  $\Theta$ - $2\Theta$  mode). It should be mentioned that for the measurements CoKa radiation was used (ratio  $\alpha_{21} = 0.5$ , divergence slit – fixed, data angle range,  $2\Theta = 10.005^\circ$ - $89.995^\circ$ , detector scan step size  $\Delta 2\Theta = 0.01^\circ$ , scan type-continuous and a scan step time  $t = 8\text{s}$ ). Analysis of the X-ray diffraction patterns was carried out using X'pert HighScore Plus software (PANalytical B.V) and Match! (Crystal Impact, Inc.) computer programme [19]. The available ICDD [20], ICSD [21], and COD [22] databases were utilized. Refinement of the structural parameters was performed with the Rietveld method [e.g. 23].

## 3. Results and discussion

Results of the X-ray diffraction analysis of BFTO ceramics sintered at different processing conditions are shown in Fig. 1. Visual inspection the diffraction patterns (Fig. 1) shows high similarity of the patterns. Therefore it was necessary to perform so called “raw data processing” that included: stripping of the alpha-2-radiation, data smoothing, peak searching, profile fitting, and correction for errors. The goal was to obtain a list of peaks ( $2\Theta$  and intensity values) with highest possible precision. It is extremely important that this step is performed as accurate as possible in order to obtain reasonable results in the search-match process later on.

Qualitative phase analysis is one goal of an X-ray diffraction experiment. Establishing which phases are present in a sample is usually the first step of a whole series of analyses. Other investigations on how much of each phase is present (quantitative phase analysis), on the texture or the stress state of solid matter and other could follow. Qualitative phase analysis is a three step procedure: (i) the search step looks for possibly matching pat-

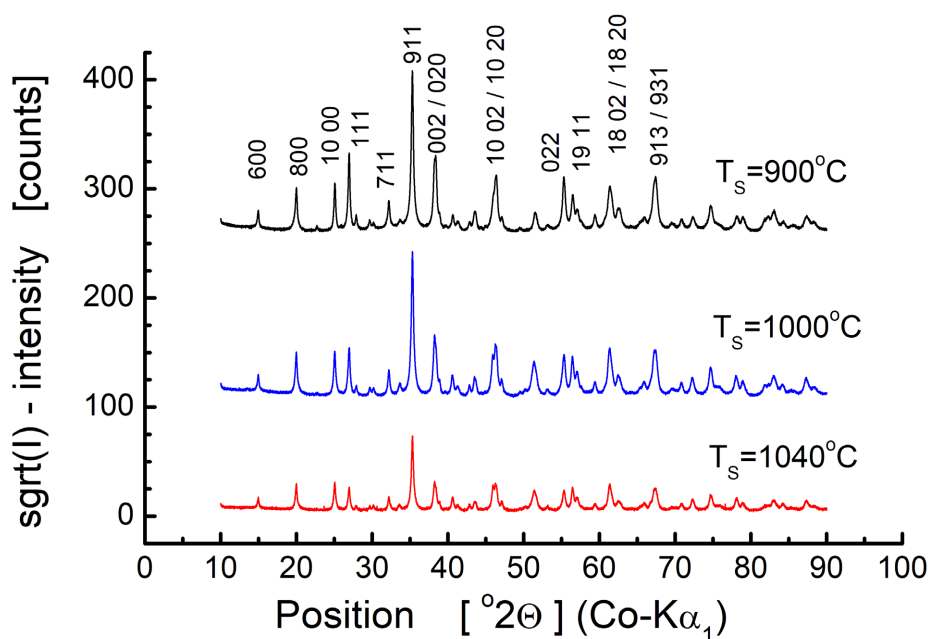


Fig. 1. Comparison of diffraction patterns of BFTO powders sintered at various temperatures:  $T_s = 900^\circ\text{C}$ ,  $T_s = 1000^\circ\text{C}$ , and  $T_s = 1040^\circ\text{C}$

TABLE 1

Global parameters of the line profile fitting

Parameters	$T = 900^{\circ}\text{C}$	$T = 1000^{\circ}\text{C}$	$T = 1040^{\circ}\text{C}$
Profile function	Pseudo Voigt	Pseudo Voigt	Pseudo Voigt
Background	Polynomial	Polynomial	Polynomial
$R$ (expected)/%	5.50377	7.63849	14.92829
$R$ (profile)/%	6.46003	7.14197	10.87721
$R$ (weighted profile)/%	8.06705	9.26152	14.82569
GOF	1.46573	1.21248	0.99313
$d$ -statistic	0.23658	0.52085	1.10947
Instrumental FWHM	Caglioti	Caglioti	Caglioti
Curve Type	function	function	function

terns in a reference pattern database, (ii) the match step inspects the best-matching patterns in much greater detail and ranks them according to score; (iii) the identification step consists of accepting a combination of well-fitting patterns, which explain the complete measured scan.

The above mentioned procedure was performed with the help of Match! computer programme [19,22]. It was established that for BFTO ceramics sintered at  $T_S = 900^{\circ}\text{C}$ ,  $T_S = 1000^{\circ}\text{C}$  and  $T_S = 1040^{\circ}\text{C}$  the major phase to be present in our samples is  $\text{Bi}_5\text{FeTi}_3\text{O}_{15}$ . This phase is described well as an entry of the COD database (COD ID: 1521427): crystal system – orthorhombic, space group  $A21am$ ; unit cell parameters:  $a = 5.4677\text{\AA}$ ,  $b = 5.4396\text{\AA}$ ,  $c = 41.2475\text{\AA}$ . The Figure-of-Merit ( $FoM$ ) – a quantity used to characterize the quality of the matching process was found  $FoM = 0.909$ ,  $FoM = 0.917$ , and  $FoM = 0.935$  respectively. Taking into consideration that all our samples were identified with high probability as single-phase  $\text{Bi}_5\text{FeTi}_3\text{O}_{15}$  compound the line profile analysis was further performed.

Line profile analysis is the extraction of microstrain and crystallite size information from a close examination of the profile width and shape. This can be done on single peaks or on a range of peaks. The line profile analysis for diffraction patterns of BFTO ceramics sintered at various processing conditions was performed and information on microstrain and crystallite size was obtained from Williamson-Hall plot [24]. Global parameters of the profile fitting are given in Table 1.

It was found that with an increase in the sintering temperature from  $T_S = 900^{\circ}\text{C}$  to  $T_S = 1000^{\circ}\text{C}$  value of the average strain increased from  $\varepsilon = 0.26(6)\%$  to  $\varepsilon = 0.35(7)\%$  respectively. Also the mean crystallite size increased from  $\langle d \rangle = 126$  nm to  $\langle d \rangle = 156$  nm. However, in case of sintering temperature  $T_S = 1040^{\circ}\text{C}$  the average strain was found  $\varepsilon = 0.21(6)\%$  and the mean crystallite size  $\langle d \rangle = 84$  nm. As an example of the

calculations performed the diffraction pattern subjected to the line profile analysis procedure (pseudo-Voigt shape function was utilised) and resulting Williamson-Hall plot for BFTO ceramics sintered at  $T_S = 1000^{\circ}\text{C}$  are shown in Fig. 2.

Detailed structural analysis, together with refinement of the elementary cell parameters (according to the Rietveld method [e.g. 23]) was performed for X-ray diffraction patterns of  $\text{Bi}_5\text{FeTi}_3\text{O}_{15}$  ceramics fabricated via solid state reaction route and pressureless sintering at  $T_S = 900^{\circ}\text{C}$ ,  $T_S = 1000^{\circ}\text{C}$  and  $T_S = 1040^{\circ}\text{C}$ . As an example of the analysis, which were carried out on the studied samples visual results of the refinement for BFTO ceramics sintered at  $T_S = 900^{\circ}\text{C}$  are shown in Fig. 3. The experimental data are represented by dots and the calculated profile by continuous line, respectively. The data angle range  $2\theta$  was limited for the purpose of improving data readability only. The vertical lines below the diffraction pattern correspond to position of the experimental (peak list) and calculated (refined) Bragg reflections of BFTO ceramics.

It is worth noting that the model structure used for refinement is  $\text{SrBi}_4\text{Ti}_4\text{O}_{15}$  structure type. To perform calculations it was

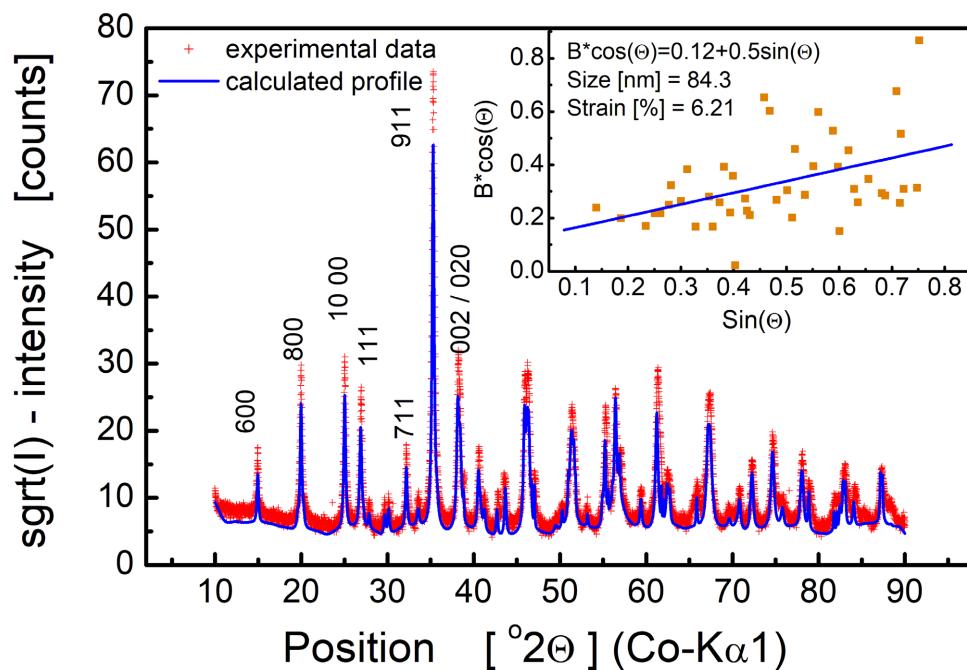


Fig. 2. Line profile analysis for diffraction pattern of BFTO sintered at  $T_S = 1040^{\circ}\text{C}$ . An insert shows Williamson-Hall plot

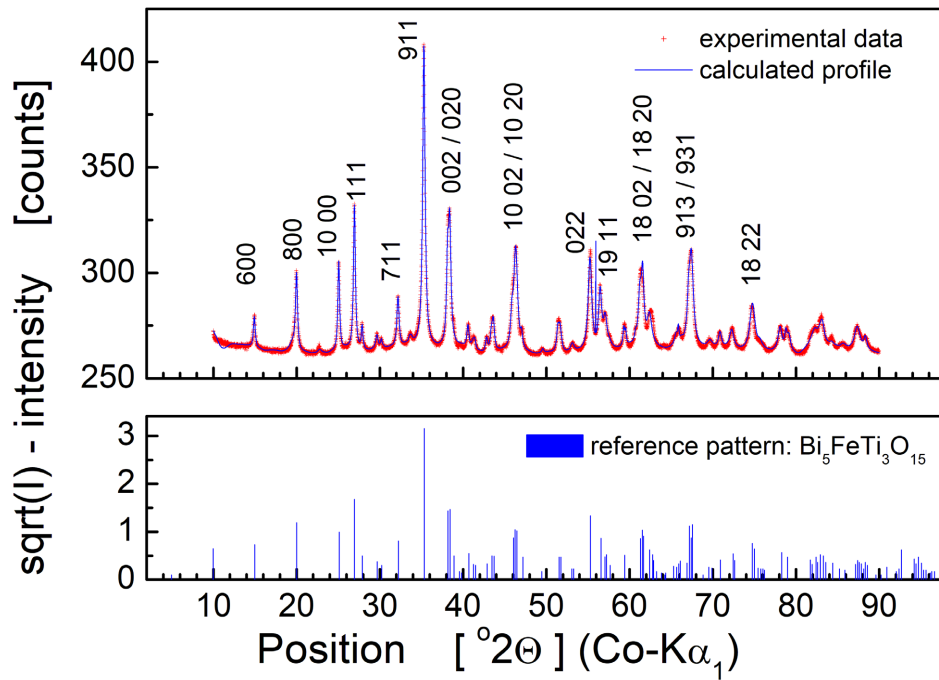


Fig. 3. Rietveld refinement for BFTO ceramics at room temperature. The experimental data are represented by *crosses* and the calculated profile by *continuous* line, respectively. BFTO ceramics was sintered at  $T_S = 900^\circ\text{C}$

transformed from setting *A21am* (original ICSD space group) to *Cmc21*. The model structure of  $\text{Bi}_5\text{FeTi}_3\text{O}_{15}$  has a PDF code 01-086-0063 and has ICSD collection code: 88869. Global parameters of the structural analysis are shown in Table 2, whereas structure parameters of the BFTO phase are given in Table 3.

TABLE 3

Structure parameters of BFTO ceramics

Relevant parameters	@ $T = 900^\circ\text{C}$	@ $T = 1000^\circ\text{C}$	@ $T = 1040^\circ\text{C}$
Space group (No.)	<i>Cmc21</i> (36)	<i>Cmc21</i> (36)	<i>Cmc21</i> (36)
Lattice parameters:			
a) Å	41.232(1)	41.278(2)	41.256(2)
b) Å	5.4392(2)	5.4434(3)	5.4437(3)
c) Å	5.4662(2)	5.4695(3)	5.4676(4)
$V/10^6 \text{ pm}^3$	1225.90200	1228.93400	1227.94300
$R$ (Bragg)/%	5.13344	13.14017	17.57985
Crystallite (rms) Strain/%	0.149	0.112	0.111
Crystallite Size/Å	783.7	528.4	570.7

TABLE 2

Global parameters of the Rietveld analysis for X-ray diffraction patterns of BFTO ceramics

Parameter	Value		
	@ $T = 900^\circ\text{C}$	@ $T = 1000^\circ\text{C}$	@ $T = 1040^\circ\text{C}$
Profile function	Pseudo Voigt	Pseudo Voigt	Pseudo Voigt
Background	Polynomial	Polynomial	Polynomial
$R$ (expected)/%	7.12543	7.73231	15.09620
$R$ (profile)/%	10.86502	17.69774	22.46896
$R$ (weighted profile)/%	14.54918	22.66386	28.62197
GOF	4.16923	8.59111	3.59471
$d$ -statistic	0.16188	0.05522	0.11177

Results of the calculations have shown that all ceramics showed an orthorhombic structure with space group *Cmc21*. It was found that the unit cell parameters of BFTO increased slightly with an increase in sintering temperature. In particular, when the sintering temperature was increased from  $T_S = 900^\circ\text{C}$  to  $T_S = 1000^\circ\text{C}$  the lattice parameters increased in amount of 0.11% (*a*), 0.08% (*b*) or 0.06% (*c*) leading to an increase in the elementary cell volume for 0.25%. On the other hand, comparison of structure parameters for BFTO ceramics sintered at  $T_S = 1000^\circ\text{C}$  and  $T_S = 1040^\circ\text{C}$  showed very small contraction of *a* and *c* elementary cell parameters with an increase in the sintering temperature.

The average crystallite strain in the ceramic samples decreased with an increase in the sintering temperature. In particular, when the sintering temperature was increased from  $T_S = 900^\circ\text{C}$  to  $T_S = 1000^\circ\text{C}$  the average crystallite strain present in the ceramic samples decreased from  $\varepsilon = 0.149\%$  to  $\varepsilon = 0.112\%$ , respectively. The average crystallite size of BFTO ceramics sintered at  $T_S = 900^\circ\text{C}$  was  $\langle d \rangle = 783\text{Å}$  whereas for  $T_S = 1000^\circ\text{C}$  the crystallite size was found  $\langle d \rangle = 528\text{Å}$ .

Comparing the results obtained by the line profile analysis and Rietveld refinement one can see slight discrepancies in values of the parameters calculated, even though global parameters of both fitting methods were similar (see Tables 1 and 2). However, it should be taken into consideration that line profile analysis calculations is valid when single phase material is subjected to the analysis. Although in the present case the probability of the single phase material was very high ( $FoM > 90\%$ ), the presence of impurities (or minor phases) cannot be excluded.

#### 4. Conclusions

Aurivillius-type bismuth layer-structured ferroelectrics with the chemical composition  $\text{Bi}_5\text{FeTi}_3\text{O}_{15}$  were synthesised and ceramics was manufactured by pressureless sintering in ambient air. X-ray studies were performed on ceramics sintered at various processing conditions. Results of the Rietveld refinement have shown that ceramics showed an orthorhombic structure with space group  $Cmc21$ . It was found that the unit cell parameters of BFTO increased slightly (for not more than 0.11%) with an increase in sintering temperature. The average crystallite strain in the samples was found to decrease with an increase in the sintering temperature from  $\varepsilon = 0.149\%$  at  $T_S = 900^\circ\text{C}$  to from  $\varepsilon = 0.112\%$  at  $T_S = 1000^\circ\text{C}$ . The average crystallite size was found to be  $\langle d \rangle = 783\text{\AA}$  for the samples sintered at  $T = 900^\circ\text{C}$ , whereas for those sintered at  $T_S = 1000^\circ\text{C}$  the crystallite size was found  $\langle d \rangle = 528\text{\AA}$ . The above mentioned results proved better crystalline perfection of the samples sintered at higher temperature.

#### Acknowledgement

The present research has been supported by Polish National Science Centre (NCN) as a research project N N507 446934.

#### REFERENCES

- [1] C. Moure, L. Lascano, J. Tartaj, P. Duran, Electrical behaviour of  $\text{Bi}_5\text{FeTi}_3\text{O}_{15}$  and its solid solutions with  $\text{CaBi}_4\text{Ti}_4\text{O}_{15}$ , *Ceramics International* **29**, 91-97 (2003).
- [2] C.A.P. De Araujo, J.D. Cuchiaro, L.D. McMillan, M.C. Scott, J.F. Scott, *Nature* **374**, 627 (1995).
- [3] R.C. Turner, P.A. Fuierer, R.E. Newnham, T.R. Srout, *Materials for high temperature acoustic and vibration sensors: a review*, *Appl. Acoustics* **41** 29-324 (1994).
- [4] T. Takenaka, K. Sakata, Grain orientation effects on electrical properties of bismuth layer-structured ferroelectric  $\text{Pb}_{(1-x)}(\text{NaCe})_{x/2}\text{Bi}_4\text{Ti}_4\text{O}_{15}$  solid solution, *J. Appl. Phys.* **55**, 1092-1099 (1984), / <https://doi.org/10.1063/1.333198>.
- [5] A. Lisińska-Czekaj, A. Lisińska-Czekaj, *Wielofunkcyjne materiały ceramiczne na osnowie tytanianu bizmutu*, Wydawnictwo Gnome, Uniwersytet Śląski, Katowice 2012.
- [6] Zhen Huang, Gen-Shui Wang, Yu-Chen Li, Rui-Hong Liang, Fei Cao, Xian-Lin Dong, Electrical properties of (Na,Ce) doped  $\text{Bi}_5\text{Ti}_3\text{FeO}_{15}$  ceramics, *Phys. Status Solidi A* **208**, 5, 1047-1051 (2011) / DOI 10.1002/pssa.201000080.
- [7] M. Krzhizhanovskaya, S. Filatov, V. Gusarov, P. Paufler, R. Bubnova, M. Morozov, D.C. Meyer, Aurivillius Phases in the  $\text{Bi}_4\text{Ti}_3\text{O}_{12}/\text{BiFeO}_3$  System: Thermal Behaviour and Crystal Structure, *Z. Anorg. Allg. Chem.* **631** 1603-1608 (2005).
- [8] N.A. Lomanova, M.I. Morozov, V.L. Ugolkov, V.V. Gusarov, Properties of Aurivillius Phases in the  $\text{Bi}_4\text{Ti}_3\text{O}_{12}-\text{BiFeO}_3$  System, *Inorganic Materials* **42**, 2 189 (2006).
- [9] B. Aurivillius, Mixed oxides with layer lattice. Structure of  $\text{BaBi}_4\text{Ti}_4\text{O}_{15}$ , *Arkiviv Khemi* **2**, 37, 519-527 (1950).
- [10] A. Lisinska-Czekaj, D. Czekaj, Z. Surowiak, J. Ilczuk, J. Plewa, A.V. Leyderman, E.S. Gagarina, A.T. Shuvaev, E.G. Fesenko, Synthesis and dielectric properties of  $\text{A}_{m-1}\text{Bi}_2\text{B}_m\text{O}_{3m+3}$  ceramic ferroelectrics with  $m = 1.5$ , *Journal of the European Ceramic Society* **24**, 947-951 (2004).
- [11] N.A. Lomanova, V.V. Gusarov, Electrical Properties of Perovskite-Like Compounds in the  $\text{Bi}_2\text{O}_3-\text{Fe}_2\text{O}_3-\text{TiO}_2$  System, *Inorganic Materials* **47**, 4, 420-425 (2011).
- [12] A. Lisińska-Czekaj, E. Jartych, M. Mazurek, J. Dzik, D. Czekaj, Dielektryczne i magnetyczne właściwości ceramiki multiferroicznej  $\text{Bi}_5\text{Ti}_3\text{FeO}_{15}$ , *Materiały Ceramiczne/Ceramic Materials* **62**, 2, 126-133 (2010).
- [13] E. Jartych, M. Mazurek, A. Lisińska-Czekaj, D. Czekaj, Hyperfine interactions in some Aurivillius  $\text{Bi}_{m+1}\text{Ti}_3\text{Fe}_{m-3}\text{O}_{3m+3}$  compounds, *Journal of Magnetism and Magnetic Materials* **322**, 51-55 (2010).
- [14] A. Lisińska-Czekaj, J. Plewa, D. Czekaj, Synthesis and structure of  $\text{Bi}_5\text{FeTi}_3\text{O}_{15}$  ceramics, *Ciência & Tecnologia dos Materiais* **29**, 210-214 (2017).
- [15] Ch.H. Hervoches, A. Snedden, R. Riggs, S.H. Kilcoyne, P. Manuel, P. Lightfoot, Structural Behavior of the Four-Layer Aurivillius-Phase Ferroelectrics  $\text{SrBi}_4\text{Ti}_4\text{O}_{15}$  and  $\text{Bi}_5\text{Ti}_3\text{FeO}_{15}$ , *Journal of Solid State Chemistry* **164**, 280-291 (2002).
- [16] M. Garcia-Guaderrama, L. Fuentes, M.E. Montero-Cabrera, A. Marquez-Lucero, and M. E. Villafuerte-Castrejon, Molten Salt Synthesis and Crystal Structure of  $\text{Bi}_5\text{Ti}_3\text{FeO}_{15}$ , *Integrated Ferroelectrics* **1**, 233-239 (2005).
- [17] M. Wu, Z. Tian, S. Yuan, Z. Huang, Magnetic and optical properties of the Aurivillius phase  $\text{Bi}_5\text{Ti}_3\text{FeO}_{15}$ , *Materials Letters* **68**, 190-192 (2012).
- [18] X.Y. Mao, W. Wang, X.B. Chen, Electrical and magnetic properties of  $\text{Bi}_5\text{FeTi}_3\text{O}_{15}$  compound prepared by inserting  $\text{BiFeO}_3$  into  $\text{Bi}_4\text{Ti}_3\text{O}_{12}$ , *Solid State Communications* **147**, 186-189 (2008).
- [19] MATCH! Version 3.6.2.121, CRYSTAL IMPACT, Postfach 1251, 53002 Bonn, Germany (URL: <http://www.crystalimpact.com/match>).
- [20] International Centre for Diffraction Data, 12 Campus Boulevard, Newton Square, PA 19073-3273 U.S.A.; (URL: <http://www.icdd.com>).
- [21] ISCD Database, FIZ Karlsruhe, (URL: <http://www.fiz-karlsruhe.de>).
- [22] IUCr/COD/AMCSD Database (URL: <http://www.crystalimpact.com/match>).
- [23] H.M. Rietveld, The Rietveld method-a historical perspective, *Austr. J. Phys.* 113-116 (1988).
- [24] G.K. Williamson, W.H. Hall, X-ray line broadening from filed aluminium and wolfram, *Acta Metallurgica* **1**, 1, 22-31 (1953). DOI: 10.1016/0001-6160(53)90006-6.